



Comparative molecular dynamics simulations of the potent synthetic classical cannabinoid ligand AMG3 in solution and at binding site of the CB1 and CB2 receptors

Serdar Durdagi^{a,b}, Heribert Reis^a, Manthos G. Papadopoulos^a, Thomas Mavromoustakos^{a,c,*}

^aInstitute of Organic and Pharmaceutical Chemistry, The National Hellenic Research Foundation, 48 Vas. Constantinou Avenue, 11635 Athens, Greece

^bDepartment of Biology, Chemistry and Pharmacy, Freie Universität Berlin, Takustr. 3, 14195 Berlin, Germany

^cDepartment of Chemistry, University of Athens, Zographou, 15784 Athens, Greece

ARTICLE INFO

Article history:

Received 31 January 2008

Revised 31 May 2008

Accepted 11 June 2008

Available online 14 June 2008

Keywords:

Cannabinoids

CB1 and CB2 receptors

Conformational analysis

Molecular dynamics simulations

Δ^8 -THC, AMG3

ABSTRACT

The C-1'-dithiolane Δ^8 -tetrahydrocannabinol (Δ^8 -THC) amphiphilic analogue (–)-2-(6a,7,10,10a-tetrahydro-6,6,9-trimethylhydroxy-6H-dibenzo[b,d]pyranyl)-2-hexyl-1,3-dithiolane (AMG3) is considered as one of the most potent synthetic analgesic cannabinoid (CB) ligands. Its structure is characterized by rigid tricyclic and flexible alkyl chain segments. Its conformational properties have not been fully explored. Structure–activity relationship (SAR) studies on classical CBs showed that the alkyl side chain is the most critical structural part for the receptor activation. However, reported low energy conformers of classical CB analogues vary mainly in the conformation of their alkyl side chain segment. Therefore, comparative molecular dynamics (MD) simulations of low energy conformers of AMG3 were performed in order to investigate its structural and dynamical properties in two different systems. System-I includes ligand and amphoteric solvent DMSO, simulating the biological environment and system-II includes ligand at active site of the homology models of CB1 and CB2 receptors in the solvent. The trajectory analysis results are compared for the systems I and II. In system-I, the dihedral angle defined between aromatic ring and dithiolane ring of AMG3 shows more resistance to be transformed into another torsional angle and the dihedral angle adjacent to dithiolane ring belonging in the alkyl chain has flexibility to adopt *gauche*± and *trans* dihedral angles. The rest of the dihedral angles within the alkyl chain are *all trans*. These results point out that wrapped conformations are dynamically less favored in solution than linear conformations. Two possible plane angles defined between the rigid and flexible segments are found to be the most favored and adopting values of $\sim 90^\circ$ and $\sim 140^\circ$. In system-II, these values are $\sim 90^\circ$ and $\sim 120^\circ$. Conformers of AMG3 at the CB1 receptor favor to establish a *cis* conformation defined between aromatic and dithiolane ring and a *trans* conformation in the CB2 receptor. These different orientations of ligand inside the binding pocket of CB1 and CB2 receptors may explain its different binding affinity in the two receptors. The results of this study can be applied to other synthetic classical CB ligands to produce low energy conformations and can be of general use for the molecules possessing flexible alkyl chain(s). In addition, this study can be useful when restraint of the alkyl chain is sought for optimizing drug design.

© 2008 Elsevier Ltd. All rights reserved.

1. Introduction

Classical and synthetic cannabinoids (CBs) are amphipathic analgesic drugs that contain a rigid segment and a flexible alkyl side

Abbreviations: CB, Cannabinoid receptor; CB1, first cannabinoid receptor; CB2, second cannabinoid receptor; GPCR, G-protein coupled receptors; MD, molecular dynamics; PME, Particle mesh Ewald; DFT, Density functional theory; 3D QSAR, three-dimensional quantitative structure–activity relationships; CoMFA, comparative molecular field analysis; CoMSIA, comparative molecular similarity indices analysis; RMSD, root mean square deviation; Δ^8 -THC, Δ^8 -tetrahydrocannabinol; AMG3, (–)-2-(6a,7,10,10a-tetrahydro-6,6,9-trimethylhydroxy-6H-dibenzo[b,d]pyranyl)-2-hexyl-1,3-dithiolane.

* Corresponding author. Tel.: +30 2107273869; fax: +30 2107273872.

E-mail addresses: tmavro@eie.gr, tmavrom@chem.uoa.gr (T. Mavromoustakos).

chain. Alkyl chain constitutes a pharmacophore segment since its structural variations cause tremendous effects on the pharmacological affinity and selectivity for the CB receptors CB1 and CB2.^{1–3} More specifically, classical CB analogues with alkyl side chains of less than five carbon atoms have limited affinity for the CB1 receptor.^{2,3} Extension of the five carbon atom chain by adding one or two carbons favors binding, while further extension is detrimental.^{2,3}

Among the synthetic analogues of Δ^8 -tetrahydrocannabinol (Δ^8 -THC); (–)-2-(6a,7,10,10a-tetrahydro-6,6,9-trimethylhydroxy-6H-dibenzo[b,d]pyranyl)-2-hexyl-1,3-dithiolane (AMG3) (Fig. 1) is considered as one of the most potent synthetic CB ligands (K_i for CB1 and CB2 receptors are 0.32 and 0.52 nM, respectively).⁴ Its conformational properties have not been fully explored yet.

Structure–activity relationships (SAR)^{4–6} and three-dimensional quantitative structure–activity relationships (3D QSAR)⁷ studies on classical CBs have revealed that the alkyl side chain is the most critical structural segment for receptor activation. However, the reported low energy conformers of classical CB analogues vary mainly in the conformation of their alkyl side chain segment. Manipulation of the flexible alkyl side chain can produce high-affinity analogues with antagonist, partial agonist, or full agonist effects.¹ Thus, information of structural and dynamical properties of alkyl side chain segment will be useful for the design of new synthetic CB analogues with enhanced activity. Moreover, a variety of classes of drug molecules contain an alkyl chain which is necessary for the drug activity (i.e., losartan, bumetanide, cannabidiol, fluvoxamine, serotonin, tianeptine, etc.; Fig. 2).

Reported drug design studies in the literature show the importance of studying the conformational analysis when restraint of the alkyl chain is sought.^{8,9} This triggered our interest to study low energy conformers of AMG3 produced using Monte Carlo (MC) simulations. Subsequently molecular dynamics (MD) simulations were performed for the selected low energy conformers of AMG3 in order to investigate its structural and dynamical properties in amphiphilic environment, because the most popular application of MD simulations is the conformational sampling, especially if experimental constraints are taken into account.¹⁰ In a drug design protocol, this method may

be very powerful tool to propose reliable conformations of small molecules in their free state and even to avoid conformational artifacts given by X-ray diffraction.¹⁰

In addition, using CB1 and CB2 receptor homology models,¹¹ the interactions of the ligand at active site of the receptor have been analyzed. Therefore, two systems have been used in MD simulations: System-I includes ligand and solvent molecules and system-II includes ligand at the binding site of the CB1 and CB2 receptors surrounded by solvent molecules. Trajectory analysis results are compared and discussed for both systems.

The selection of the lowest energy conformation of the bioactive conformation of the template molecule and the superimposition of all molecules on template compound are the two most critical steps in the 3D QSAR studies, especially for comparative molecular field analysis (CoMFA)¹² and comparative molecular similarity indices analysis (CoMSIA)¹³ methodologies. Comparative MD simulations of ligand in solution and at binding site of the receptor lead to understand its favored conformation inside the receptor and may help to improve the alignment procedure. Thus, applications of MD simulations in solution and at binding site of the receptor can provide statistically more reliable models.^{14–16} Furthermore, since trajectory analysis has been performed for both CB1 and CB2 receptors, results can be useful for synthetic chemists to produce more selective CB compounds.

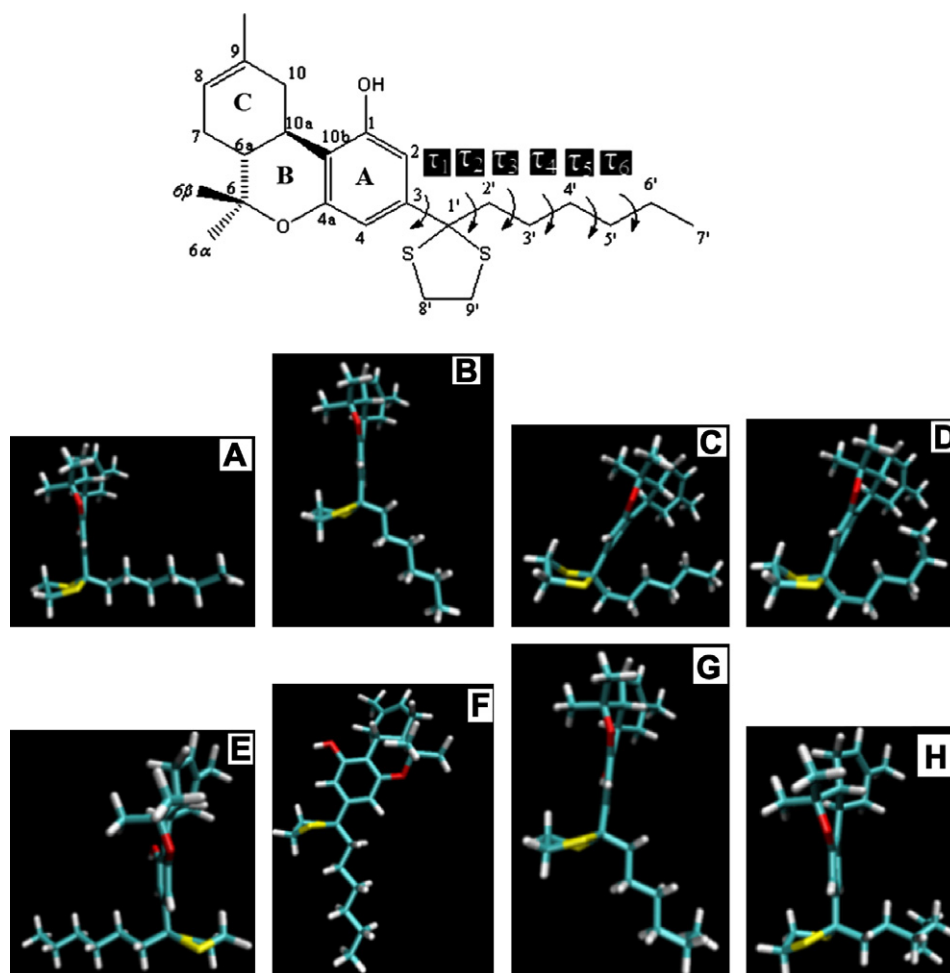


Figure 1. (i) Molecular structure of AMG3 and its derived 3D low energy conformers A–H. Dihedral angles of the alkyl side chain are assigned on the top structure (τ_1 , C2–C3–C1'–C2'; τ_2 , C3–C1'–C2'–C3'; τ_3 , C1'–C2'–C3'–C4'; τ_4 , C2'–C3'–C4'–C5'; τ_5 , C3'–C4'–C5'–C6'; τ_6 , C4'–C5'–C6'–C7').

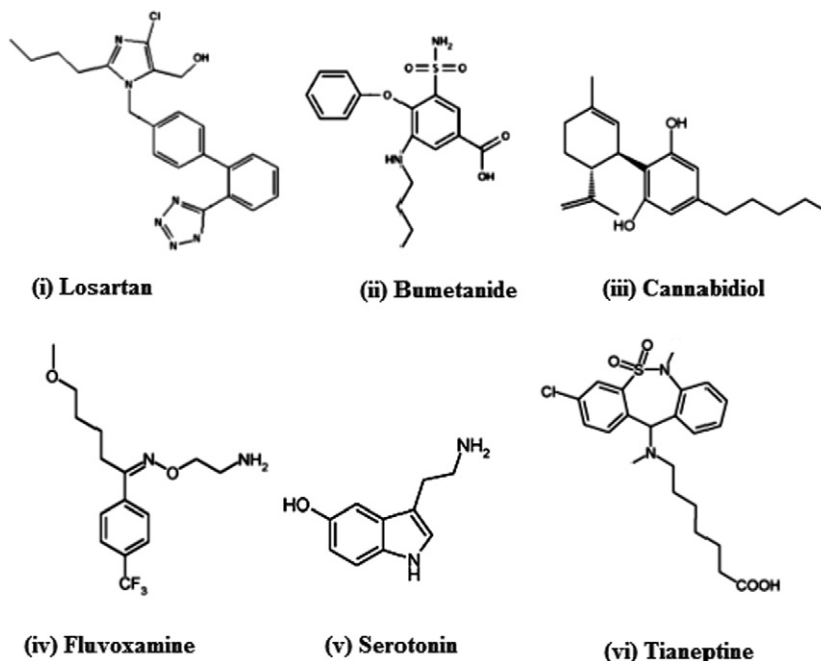


Figure 2. The following drug molecules containing an alkyl chain are necessary for the drug activity: (i) losartan; (ii) bumetanide; (iii) cannabidiol; (iv) fluvoxamine; (v) serotonin; and (vi) tianeptine.

2. Methods

2.1. MC simulations

MC simulations using random sampling search method were performed with QUANTA/CHARMm software¹⁷ in order to investigate a complete conformational space for the AMG3. The MC simulations created 1000 conformers, and these conformers are grouped into eight clusters based on torsional angle values. From each cluster, the lowest-energy conformer was selected for further analyses.

2.2. Geometry optimization of conformations in gas phase

Selected conformers from MC simulations were subjected to full geometry optimization in gas phase using a combination of the standard Tripos molecular mechanic (MM) force field of the Sybyl molecular modeling package¹⁸ with Powell energy minimization algorithm,¹⁹ Gasteiger–Hückel charges²⁰ and 0.001 kcal/mol Å energy gradient convergence criterion. Ab initio calculations were applied with Gaussian 98²¹ and for all calculations B3LYP/6-31G^{*22,23} level of density functional theory (DFT) was used.

2.3. Topologies of AMG3 conformers

The coordinates of AMG3 conformers were submitted to PROD-RG²⁴ algorithm to obtain Gromacs topologies. No new atom types are included, thus the atom charges and force constants for AMG3 conformers are all defined in gmX force field.²⁵

2.4. Simulation details

(i) *System-I (ligand in a solvent environment)*: The MD simulations were performed with GROMACS 3.3.1 software package²⁶ using gmX force field. Canonical NVT ensemble at 300 K was used with periodic boundary conditions, and the temperature was kept constant by the Berendsen thermostat.²⁷ Electrostatic interactions were calculated using the particle mesh Ewald method.²⁸ Cutoff

distances for the calculation of Coulomb and van der Waals interactions were 1.0 and 1.4 nm, respectively. The cubic elementary box contained AMG3 ligand and DMSO molecules corresponding to the range of density of 0.8–1.05 g/cm³. The size of the cubic box which corresponds to each conformer, the number of DMSO molecules and the resulted densities are presented in Table 1. Prior to the dynamics simulation, energy minimization was applied to the full system (AMG3 molecule and solvent DMSO molecules) without constraints using the steepest descent integrator for 5000 steps with the initial step size of 0.01 Å (the minimization tolerance was set to 100 kJ/(mol.nm)). The system was then equilibrated via a 20 ps MD simulations at 300 K. Finally, a 1 ns simulations was performed at 300 K with a time step of 0.5 fs. (ii) *System-II (ligand localized at the active site of the receptors in a solvent environment)*: The cubic box (83.7 Å³) including total of 18,884 atoms was used for MD simulations of ligand at the binding site of the CB1 receptor and a cubic box (81.5 Å³) including total of 17,345 atoms was used for the MD simulations of ligand at the binding site of the CB2 receptor. Same parameters for MD simulations of system-I have been kept identical except the time step, equilibration, and simulation time. Due to complexity of the system, 50 ps equilibration and 2.5 ns simulation time have been applied with 2 fs time step. Effect of solvent on conformations was also examined changing the solvent from DMSO to water environment. Visualization of the dynamics trajectories was performed with

Table 1

Size of cubic boxes, number of used DMSO molecules, and resulted densities for each conformer at system-I

Conformer	No. of DMSO molecules	Size of cubic box (Å)	Density (g/ml)
A	194	29.30	1.03
B	217	33.21	0.80
C	197	29.19	1.05
D	193	29.21	1.03
E	188	31.62	0.80
F	205	32.30	0.95
G	191	31.74	0.80
H	194	29.72	0.99

the VMD software package.²⁹ Origin 6.0 program³⁰ was used for dihedral angles versus time plots and statistical calculations. Parameters used in the GROMACS program are reported in the Supporting Information.

3. Results

3.1. MD simulations on system-I

The application of MC analysis, which allows full angular window specification and random change of all flexible dihedral angles responsible for the flexibility, generated 1000 conformers of AMG3. These conformers are grouped within the eight families based on torsional angles of conformers, and from each family a lowest energy conformer is selected. Selected conformers are further optimized using Tripos MM force field. Optimized conformers are shown in Figure 1. Their dihedral angle values of rotatable bonds at the alkyl chain and standard deviation values for each dihedral angle are summarized in Table 2.

MD simulations were performed with the GROMACS 3.3.1 software package to all presented conformers using amphoteric solvent DMSO. DMSO is selected as solvent because it provides an amphiphilic environment, which mimics physiological conditions and therefore it is appropriate for investigating biological structures.³¹

MD simulations have shown that, τ_3 – τ_6 have optimal dihedral angle value at $\sim 180^\circ$ for all of the presented conformers. Thus, even some perturbation around this angle was observed at certain intervals, the dihedral angle of $\sim 180^\circ$ finally preserved.

During the simulation, all dihedral angle values kept their initial values for the conformers **A**, **B**, and **E** except the τ_2 . It has dynamic equilibrium structures with *gauche* \pm and *trans* conformations. Changes of the dihedral angles in the alkyl chain during the simulation for the conformers **A**, **B**, and **E** are shown in Figure 3. Torsional angle of τ_2 adopts mainly *gauche* \pm and *trans* dihedral angles for conformer **A**; *gauche* $-$ and *trans* dihedral angles for conformer **B**; and *gauche* $+$ and *trans* dihedral angles for conformer **E**. Thus, for these conformers, different geometries are in dynamic equilibrium during the simulation. For example, (i) conformer **A** can keep its initial conformation; (ii) it can be transformed to conformer **B**; and (iii) it can be transformed to a new conformation which has same dihedral angle values of conformer **A**, except τ_2 which has a *gauche* $-$ conformation (it is called conformer **A'** and it is shown in Fig. 4 (on the left)). Conformer **B** can keep its initial state or it can change its conformation to conformer **A'** during the simulation. Conformer **E** can keep its initial conformation or it can be transformed to a new conformation which has same dihedral angle values of conformer **E**, except τ_2 which has a *gauche* $-$ conformation (it is called conformer **E'** and it is shown in Figure 4 (on the middle)).

Table 2

Values of dihedral angles corresponding to the alkyl chain part for the selected low energy conformers of AMG3 derived by MC and further optimization with Tripos MM force field

Conformer	τ_1 (degree)	τ_2 (degree)	τ_3 (degree)	τ_4 (degree)	τ_5 (degree)	τ_6 (degree)
A	73.2	57.8	178.9	179.7	180.0	180.0
B	81.9	181.0	179.8	180.0	180.0	180.0
C	54.8	65.2	294.3	191.3	181.8	180.2
D	55.2	69.1	301.2	190.9	176.4	63.7
E	257.6	58.0	178.6	179.7	180.0	180.0
F	187.0	177.1	176.6	179.5	179.9	180.0
G	82.2	181.0	179.9	180.5	185.7	296.4
H	103.4	302.9	182.5	186.5	302.0	302.3
Std. Dev.	72.4	88.9	54.9	5.2	43.0	77.7

Wrapped conformations of alkyl chain in conformers **C** and **D** were quickly lost and are transformed to linear conformers, where they remained intact during the simulation. Torsional angle of τ_1 kept its initial value during simulation for the conformers **C** and **D**; however, τ_2 populated mainly at *gauche* $+$ and *trans* for conformer **C**; *gauche* \pm and *trans* for conformer **D**. Change of the τ_2 values versus time throughout simulations have been shown for conformers **C** and **D** in Figure 5. Last four rotatable bonds in alkyl chain (τ_3 – τ_6) of conformers **C** and **D** were populated dominantly at *trans* conformation, thus they were transformed to conformers **A**, **A'**, and **B**.

Both τ_1 and τ_2 values of the alkyl chain changed during the simulation for conformer **F**. *Trans* conformation of τ_1 is converted to *gauche* $-$ conformation, and τ_2 is populated dominantly at *trans* and at *gauche* $-$ for conformer **F** (Fig. 6). Thus, it is transformed to conformer **E'** or a new conformation which is called conformer **F'** (its τ_1 and τ_2 dihedral angles adopt *gauche* $-$ and *trans* conformations, respectively, and the rest of the four rotatable bonds (τ_3 – τ_6) in alkyl chain have *trans* conformation). Conformer **F'** has been shown in Figure 4 (on the right).

Conformer **G** kept its initial dihedral conformations except τ_2 and τ_6 ; τ_2 populated mainly at the *trans* and *gauche* $-$ conformations and τ_6 is transformed from *gauche* $-$ to *trans* conformation. Thus, conformer **G** is transformed to conformers **A'** and **B**. Torsional angles τ_1 and τ_2 of conformer **H** are populated mainly at *gauche* \pm and at *trans*, *gauche* $-$ conformations, respectively. Thus, conformer **H** can be transformed to conformers **A'**, **B**, **E'** and **F'** throughout the simulation.

Therefore, our MD results for system-I showed that there are six favored interconvertible conformations: **A**, **A'**, **B**, **E**, **E'** and **F'**. Novel conformers (**A'**, **E'**, and **F'**) which are derived from MD simulations of system-I were superimposed with their corresponding conformations (**A**, **E**, and **F**) in Figure 7. Dihedral angle values of the alkyl chain of favored conformations derived from MD after geometry optimization using MM and QM methods in gas phase and root mean square deviation (RMSD) values between MM and QM results for each conformer are summarized in Table 3. These conformers form two favored plane angles defined between rigid and flexible segments, and adopt values of $\sim 90^\circ$ and $\sim 140^\circ$. Planes for the rigid and flexible segments of AMG3 are defined by the four atoms (C1, C2, C4, and C4a) in ring A and by the four atoms (C1', C7', and sulfur atoms) of alkyl side chain (Fig. 8). Formed plane angles of favored conformations after MM and QM geometry optimizations and their relative energies are compared in Table 4. Relative energy differences are used for clarity and are defined on lowest total energy of conformers calculated by MM and QM methods. The lowest energy conformers (**A'** for QM and **E'** for MM methods) are arbitrarily assigned with zero potential energy and relative energies of other conformers are calculated. Both MM and QM calculations showed that, all favored conformations derived from MD have similar relative energies; however conformers which form perpendicular plane angle between rigid and flexible segments have slightly lower energy (~ 1 kcal/mol) than corresponding plane angle of $\sim 140^\circ$.

3.2. MD simulations on system-II

In order to analyze the effects of critical amino acid residues at the active site of CB receptors to the conformational properties of ligand, MD simulations of AMG3 in the homology models of CB1 and CB2 receptors have been carried out. Three-dimensional (3D) models of the CB receptors were constructed by several groups (Tuccinardi et al.¹¹ and Shim et al.³²) with a molecular modeling procedure using the X-ray structure of bovine rhodopsin³³ as the initial template structure and taking into account the available site-directed mutagenesis data. These research groups studied dif-

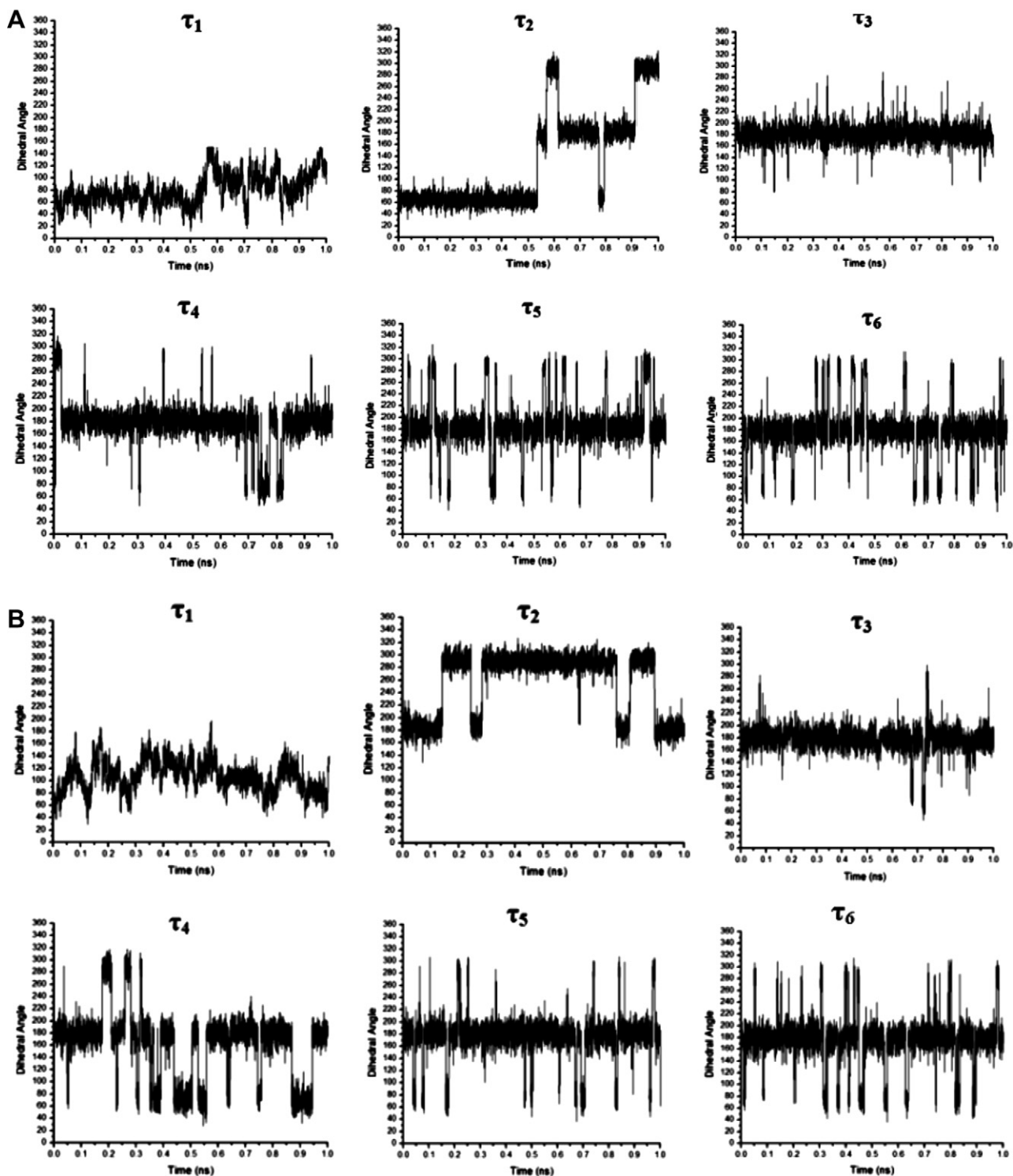


Figure 3. Changes of dihedral angle values in the alkyl chain of AMG3 throughout the MD simulations of system-I for conformers A, B, and E.

ferent ligands of CB classes; however, they found that all CBs studied interact at an active site with similar homologies.¹⁶

Prior to the MD simulations, molecular docking studies have been applied using FlexX docking algorithm of SYBYL molecular modeling package¹⁸ to the obtained stable conformations of AMG3 (A, A', B, E, E', and F') derived from MD simulations of system-I. FlexX is a computational docking program that uses an efficient incremental construction algorithm in order to optimize the interaction between a flexible ligand and rigid binding site resi-

dues of a receptor. The more recent 3D models of the CB receptor were used for the molecular docking studies; however, the binding site residues are determined considering both models mentioned above. Figure 9 illustrates the docked conformers of AMG3 inside the CB1 and CB2 receptors. Docking solutions of each conformer were settled to produce maximum of 30 different binding modes. Population analysis of docking modes for both of CB1 and CB2 receptors showed that the conformer B has the highest propensity at the binding site. The coordinates of best docked (best binding

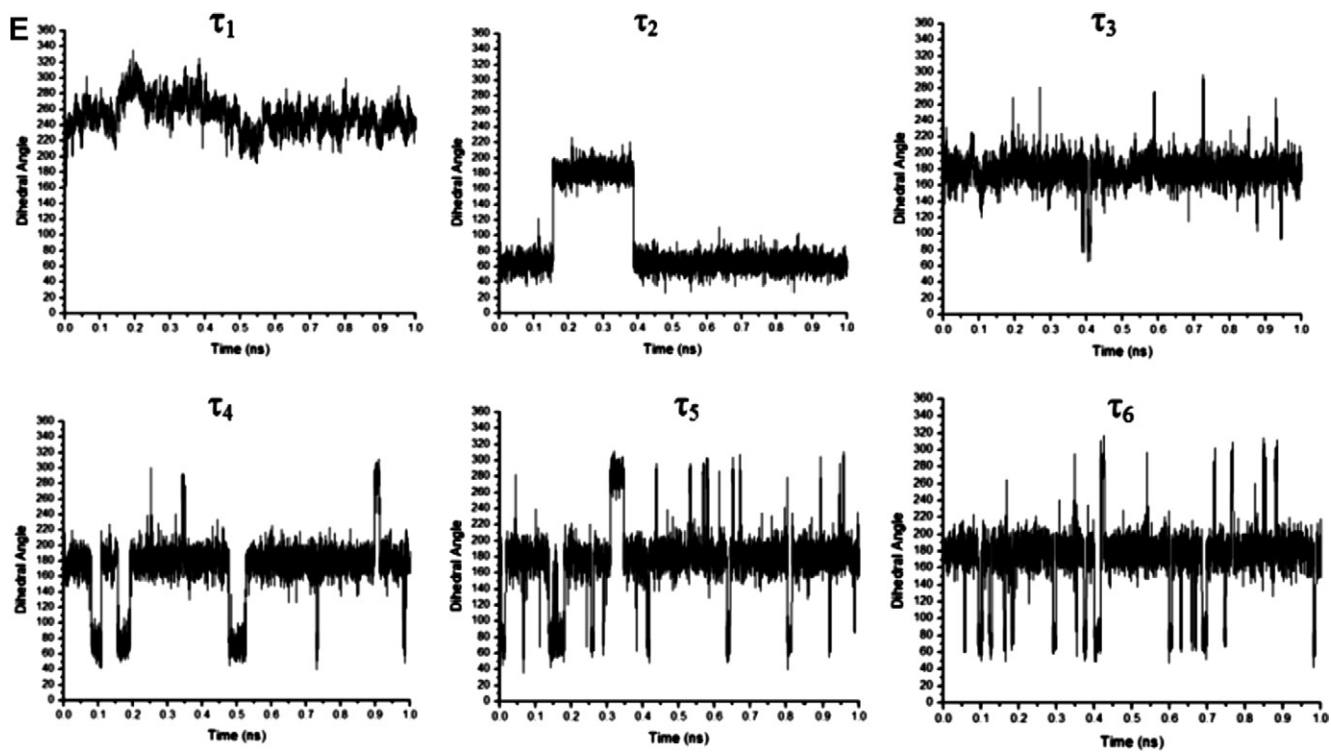


Figure 3 (continued)

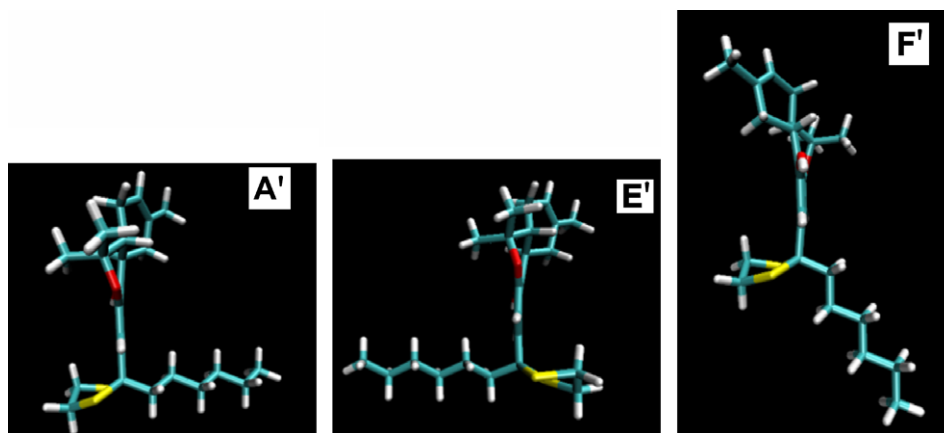
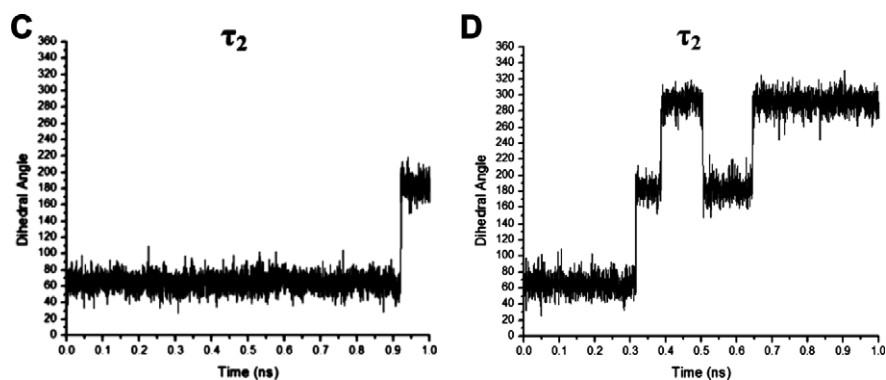


Figure 4. MD simulations of AMG3 in system-I derived new conformations: conformers A' (on the left), E' (on the middle) and F' (on the right).

Figure 5. Change of the τ_2 throughout the MD simulations for conformers C and D.

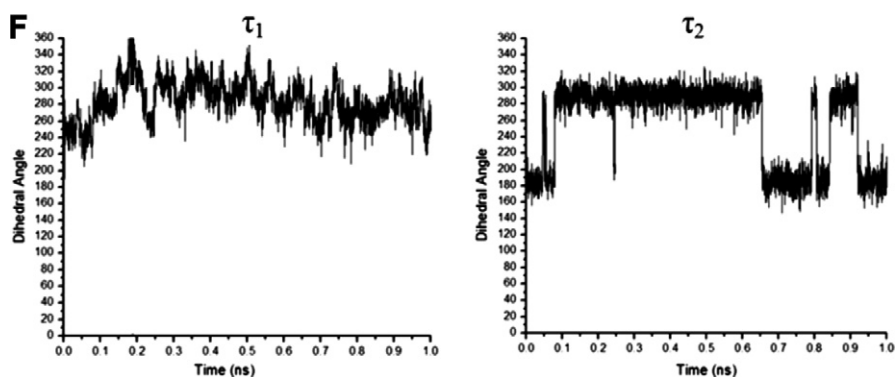


Figure 6. Changes of the τ_1 and τ_2 throughout the MD simulations for conformer F.

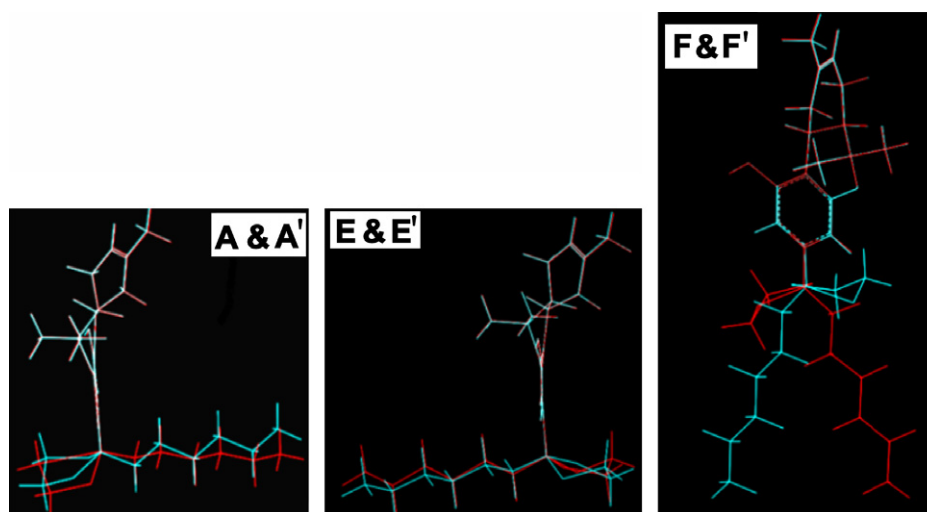


Figure 7. Superimposition of conformers A and A' (on the left), E and E' (on the middle), F and F' (on the right) (initial and derived structures from MD simulations are showed with red and blue colors in figure, respectively).

Table 3

Values of dihedral angles corresponding to the alkyl chain part for favored low energy conformers of AMG3 derived by applying MD and further optimization with Tripos MM force field and QM method with DFT/B3LYP/6-31G* level

Conformer	τ_1 (degree)		τ_2 (degree)		τ_3 (degree)		τ_4 (degree)		τ_5 (degree)		τ_6 (degree)		RMSD
	MM	QM											
A	73.2	63.3	57.8	61.1	178.9	181.1	179.7	180.5	180.0	180.2	180.0	180.1	4.37
A'	103.9	125.6	302.1	297.3	181.2	178.5	180.2	179.2	180.0	179.4	180.0	179.6	9.15
E	257.6	250.5	58.0	60.9	178.6	180.8	179.7	180.1	180.0	180.1	180.0	180.0	3.26
E'	282.8	299.2	302.2	298.3	181.4	178.7	180.3	179.9	180.0	179.9	180.0	180.0	6.97
F	187.0	187.2	177.1	175.6	176.6	177.8	179.5	179.6	179.9	179.5	180.0	180.1	0.81
F'	274.6	272.8	179.3	184.1	180.2	186.7	180.0	180.9	180.0	180.7	180.0	180.0	3.41

RMSD values between MM and QM results are also shown in table.

score) mode of conformer of AMG3 at the CB1 and CB2 receptors have been used for MD simulations. Because of consistency in comparison of system-I and system-II, we used the same polar aprotic solvent, DMSO. The effect of solvent was also examined by applying simulations in water. The results showed that the more polar solvent water did not exert considerable differential effect on the conformation.

Changes of the dihedral angles that define the alkyl chain of AMG3 at the CB1 receptor during the simulation are shown in Figure 10. MD simulations have shown that τ_1 has been decreased gradually from *gauche+* to *cis* conformation for the AMG3 ligand. Dihedral angle τ_2 has dynamic equilibrium conformers with two possible values at *gauche+* and *trans*. Differently from MD simula-

tions results of system-I, τ_4 of AMG3 at the active site of the CB1 receptor model adopts two values of torsional angle: *trans* and *gauche-*. Dihedral angle values of τ_3 , τ_5 , and τ_6 adopt *trans* conformations for the AMG3 at the CB1 receptor model. The obtained conformers are called as I, J, K, and L and are shown in Figure 11 (adopted values of their dihedral angles $\tau_1 - \tau_6$ are provided in figure legend, correspondingly).

Changes of the dihedral angles in the alkyl chain of AMG3 at the CB2 receptor during the simulations are shown in Figure 12. MD simulations have shown that $\tau_3 - \tau_6$ dihedral angles adopt optimal value of *all trans*. Torsional angle τ_1 shows a gradual increase from *gauche+* to *trans* and τ_2 has dynamic equilibrium conformers with two possible *trans* and *gauche-* conformations. Thus, two different

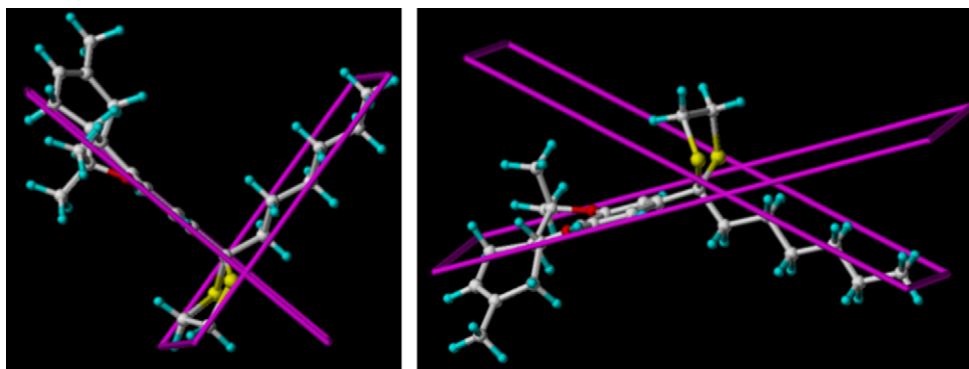


Figure 8. Two possible plane angles between rigid and flexible segments of AMG3; $\sim 90^\circ$ (on the left) and $\sim 140^\circ$ (on the right). Planes for the rigid and flexible segments of AMG3 are defined with four atoms (C1, C2, C4, and C4a) in ring A and with four atoms (C1', C7', and sulfur atoms) in alkyl side chain.

Table 4
Plane angles between rigid and flexible segments and relative energies of favored conformations in system-I

Conformer	MM-plane angle (degree)	QM-plane angle (degree)	MM-relative energy (kcal/mol)	QM-relative energy (kcal/mol)
A	87.0	89.04	0.16	0.16
A'	87.5	87.51	0.23	0.00
E	88.8	86.58	0.09	0.15
E'	89.4	91.35	0.00	0.60
B	137.9	135.49	1.03	1.40
F'	141.4	137.86	0.81	1.30

In table, relative energies (differences of total energies based on lowest total energy of conformers calculated by MM and QM methods; the lowest energy conformer of AMG3 with MM and QM methods is found to be **E'** and **A'**, respectively) have been used instead at total energies for clarity.

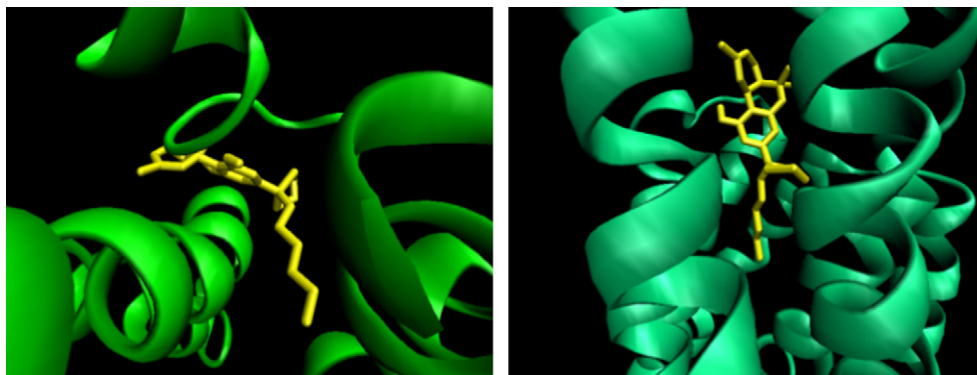


Figure 9. Docked conformers of AMG3 inside the CB1 (on the left) and CB2 receptors (on the right).

conformations of AMG3 can be adopted at the binding site of the CB2 receptor. One of them (*all trans* dihedral angles for alkyl chain) has same dihedral angle values with conformer **F** and other conformer is a novel one and has *gauche*- dihedral angle for τ_2 and rest of the dihedral angles in alkyl chain are *trans*. This conformer called conformer **M** and is shown together with conformer **F** in Figure 13.

Conformers **J**, **K**, and **M** form a perpendicular plane angle between flexible and rigid segments of AMG3, whereas, conformers **F**, **I**, and **L** form a plane angle value of $\sim 120^\circ$.

Although the CB1 and CB2 receptors exhibit a very high sequence homology which rises to 68% in the transmembrane (TM) regions, there are certain behavior differences of AMG3 conformers at the binding sites of receptors. One of the main differences between the MD simulations of ligand at the CB1 receptor and at the CB2 receptor is the different behavior of the dihedral angle of τ_1 . In the CB1 receptor, there is a high propensity of τ_1 to establish a *cis* conformation, however, in the CB2 receptor, it prefers to have a *trans* conformation. Figure 14

shows the superimposition of conformer **I**, which prefers a *cis* dihedral angle for τ_1 at CB1 receptor; and conformer **F** which prefers a *trans* dihedral angle for τ_1 at CB2 receptor. As clearly shown in Figure 14, the orientation of the alkyl chain due to τ_1 of AMG3 inside the CB1 and CB2 receptors differs. The dihedral angle values of $\tau_3 - \tau_6$ adopt an optimal value at *all trans*, even some perturbation around this angle is observed at certain intervals, at the CB2 receptor. The same value was observed for $\tau_3 - \tau_6$ when MD simulations are applied to receptor-free simulations. However, MD simulations for the AMG3 at the CB1 receptor showed that torsional angle value for the τ_4 populated dominantly at *trans* and *gauche*- conformations, therefore both linear and wrapped conformations of alkyl side chain of AMG3 can be obtained in the CB1 receptor.

It is well-known that, different conformational rearrangements of third and sixth TMs of G protein coupled receptors (GPCR) determine the activation of CBs. In CB2 receptor, alkyl side chain of AMG3 conformers align parallel in the ligand recognition part of TM3, while in the CB1 receptor they align almost perpendicular.

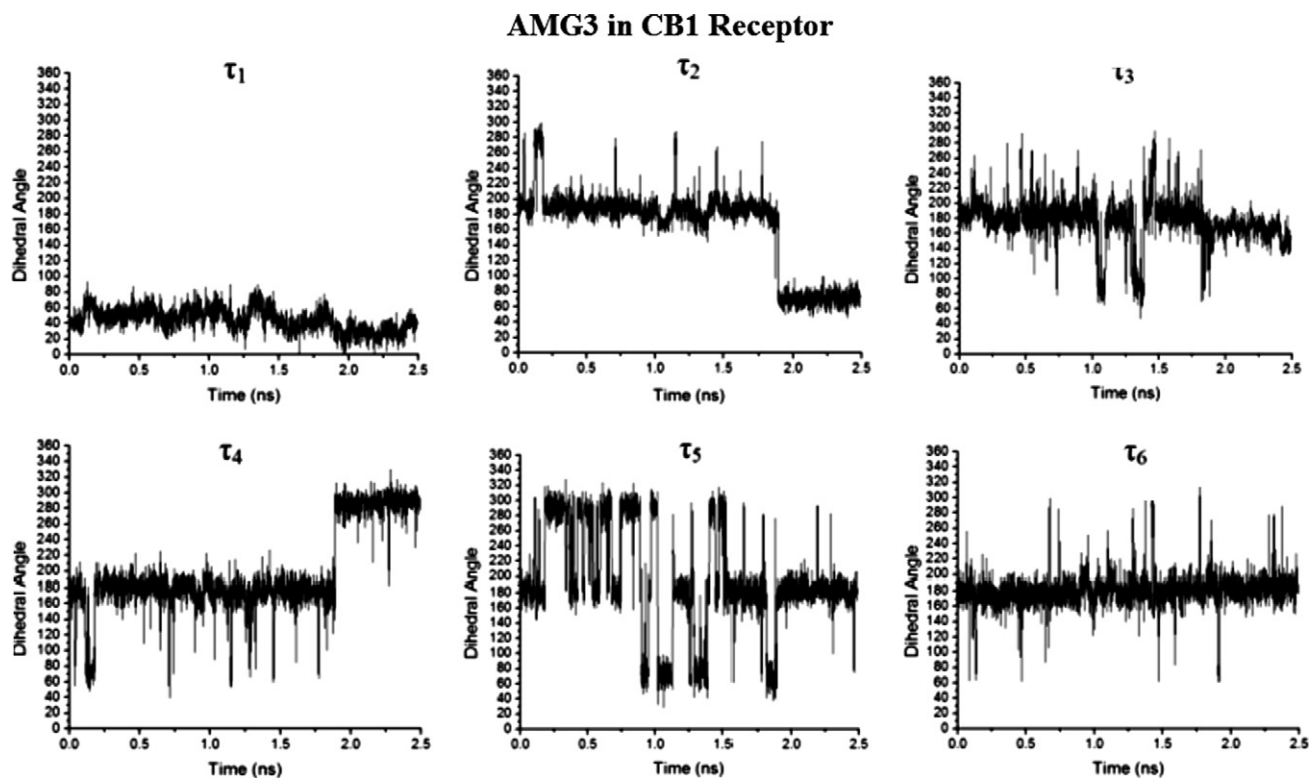


Figure 10. Dihedral angle flexibility of the alkyl chain of AMG3 when binds at the active site of CB1 receptor throughout the simulation of molecular motion.

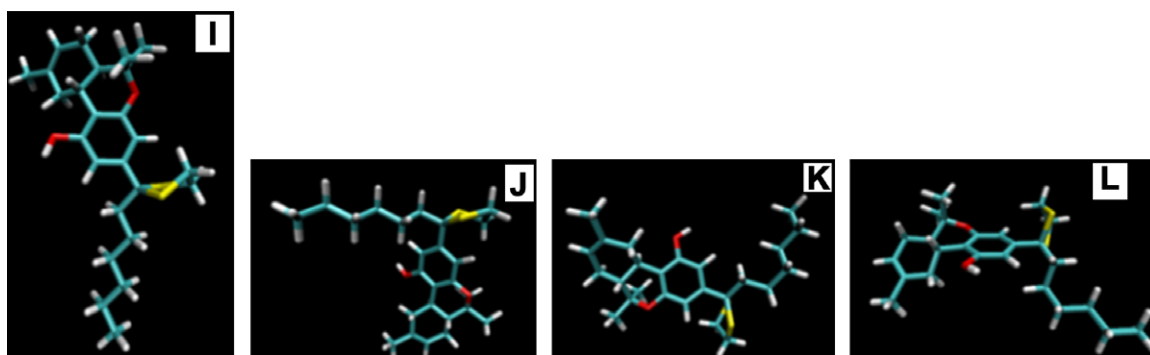


Figure 11. Conformers I, J, K, and L derived throughout the simulations of AMG3 at the binding site of the CB1 receptor model. Their adopted dihedral angles for $\tau_1 - \tau_6$ at the alkyl chain have following values, respectively, conformer I: *cis/trans/trans/trans/trans/trans*; conformer J: *cis/gauche+/trans/trans/trans/trans*; conformer K: *cis/trans/trans/gauche-/trans/trans*; and conformer L: *cis/gauche+/trans/gauche-/trans/trans*.

This observation may help to understand the selectivity of CB ligands for the CB1 and CB2 receptors.

4. Conclusions

In this study, the conformational properties of the highly active CB analogue AMG3 'in solution' and 'at the active site of CB1 and CB2 receptors' have been explored. The MD simulations of 'in solution' trajectory analysis showed that the dihedral angle defined between aromatic and dithiolane ring of the alkyl side chain of AMG3 shows more resistance to be transformed to another torsional angle because the heterocyclic part interacts with the ring A of the rigid segment and leads to restriction of the rotation. The $\tau_3 - \tau_6$ dihedral angles are transformed to optimal dihedral angle value of *all trans* conformations. Thus, the wrapped conformations (i.e., conformers C and D) are dynamically less probable in solution than the linear conformations. The τ_2 dihedral angle belonging to the al-

yl chain has dynamic equilibrium structures with three possible interconvertible dihedral angle of *gauche±* and *trans* conformations. Therefore, it appears that the second dihedral angle is the most critical dihedral angle in solution for producing different low energy conformations. Possible of these conformations are A, A', B, E, E' or F' and their formed plane angles between rigid and flexible segments are $\sim 90^\circ$ and $\sim 140^\circ$.

Both of MM and QM geometry optimization calculations showed that favored conformations of AMG3 derived from MD have similar relative energies; however, conformers which have perpendicular plane angle (between rigid and flexible segments) have slightly lower relative energies than those that adopt a plane angle of $\sim 140^\circ$.

The obtained results suggest that synthetic analogs incorporating restraints (multiple bonds or rings) at different positions of alkyl chain may be of importance to be synthesized. Especially, such synthetic analogs are important if they restrict the favorable angles

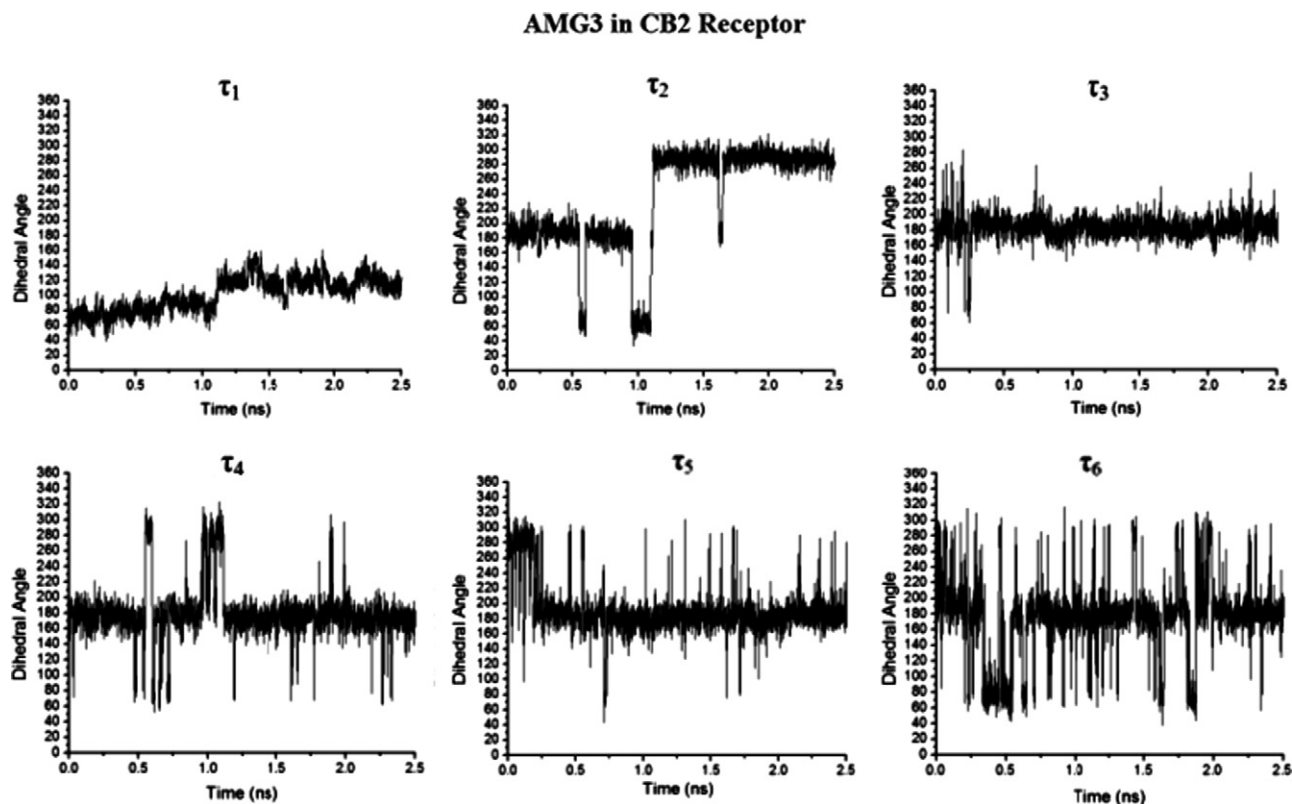


Figure 12. Dihedral angle flexibility of the alkyl chain of AMG3 when binds at the CB2 receptor throughout the simulation of molecular motion.

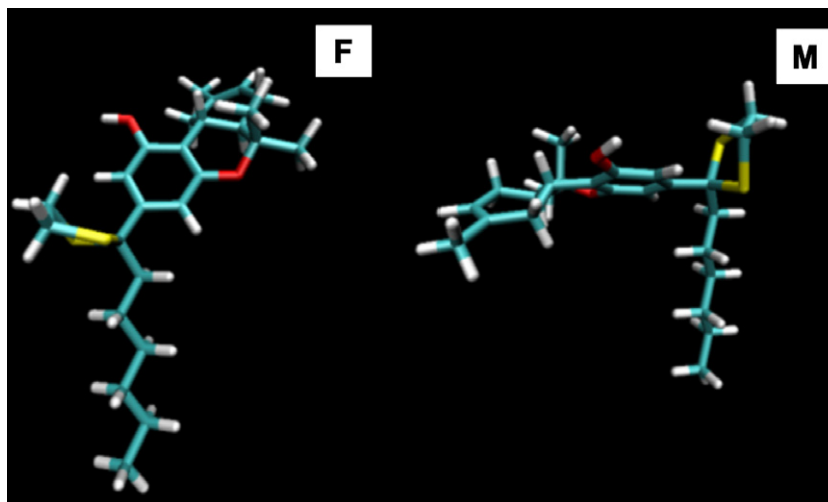


Figure 13. Conformers **F** and **M** derived throughout the simulations of AMG3 at the binding site of the CB2 receptor model. Their adopted dihedral angles for $\tau_1 - \tau_6$ at the alkyl chain have following values, respectively, conformer **F**: *trans/trans/trans/trans/trans/trans*; and conformer **M**: *trans/gauche-/trans/trans/trans/trans*.

and avoid the perturbation effects around the favorable dihedral angle.

The MD simulations ‘at active site of the receptor’ trajectory analysis results showed that, conformers form perpendicular and $\sim 120^\circ$ plane angles between flexible and rigid segments. In the CB1 receptor, ligand can adopt both *cis* and *trans* conformations; however, in CB2 receptors, conformers prefer to adopt only *trans* conformations for $\tau_3 - \tau_6$. Conformers of AMG3 at the active site of the CB1 receptor prefer to establish a *cis* conformation for the τ_1 , but *trans* conformation at the active site of the CB2 receptor.

This leads to different orientations of conformers of CB ligands inside the receptor and may explain their differences in activity and may trigger the interest to the synthetic chemists to produce more selective compounds.

Moreover, our detailed MD analysis of selected AMG3 conformers clarified the controversial results in literature for the proposed low energy conformations of classical CBs in solution. Up to date, only perpendicular and wrapped conformations are thought as the lowest energy conformations of classical CBs. However, our MD results showed that wrapped conformations are not stable

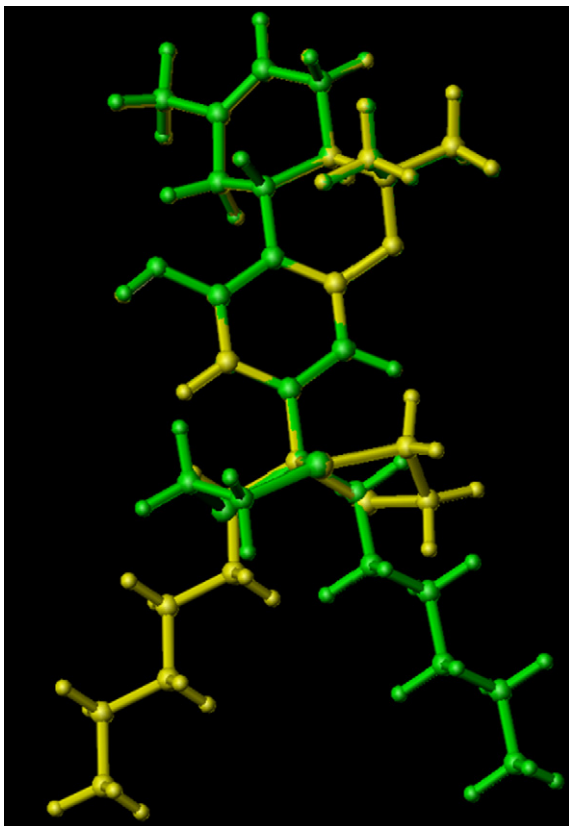


Figure 14. Superimpositions of derived conformers I and F show clearly the different orientations of ligand at the active site of the CB1 and CB2 receptors.

during the simulation, in solution. In addition, to our knowledge, it is the first time that a linear-like ($\sim 140^\circ$ between flexible alkyl chain and rigid segments) conformation of CBs is shown to possess low energy conformation in solution. The results of this study are not limited to CB ligands but it can be of general use in drug design. Moreover, several ideas can be generated through this analysis aiming in the optimization of the drug design (i.e. consideration of a synthetic effort in which other positions of alkyl chain are substituted or restrained which avoid perturbations on the optimal dihedral angle).

Acknowledgements

This work was financially supported by the European Union within 6th Framework Programme-Marie Curie Actions (Project: EURODESYS-MEST-CT-2005-020575). We gratefully acknowledge Prof. A. Martinelli (Molecular Modeling and Virtual Screening Laboratory, Department of Pharmaceutical Science, University of Pisa) for sharing their constructed models of CB1 and CB2 receptors.

Supplementary data

Supplementary data associated with this article can be found, in the online version, at doi:10.1016/j.bmc.2008.06.019.

References and notes

- Reggio, P. H. *Curr. Pharm. Des.* **2003**, *9*, 1607.
- Thakur, G. A.; Duclos, R. I., Jr.; Makriyannis, A. *Life Sci.* **2005**, *78*, 454.
- Khanolkar, A. D.; Palmer, S. L.; Makriyannis, A. *Chem. Phys. Lip.* **2000**, *108*, 37.
- Papahatjis, D. P.; Kourouli, T.; Abadji, V.; Goutopoulos, A.; Makriyannis, A. *J. Med. Chem.* **1998**, *41*, 1195.
- Razdan, R. K. *Pharmacol. Rev.* **1986**, *38*, 75.
- Makriyannis, A.; Rapaka, R. S. *Life Sci.* **1990**, *47*, 2173.
- Durdagi, S.; Kapou, A.; Kourouli, T.; Andreou, T.; Nikas, S. P.; Nahmias, V. R.; Papahatjis, D. P.; Papadopoulos, M. G.; Mavromoustakos, T. *J. Med. Chem.* **2007**, *50*, 2875.
- Zoumpoulakis, P.; Daliani, I.; Zervou, M.; Kyrikou, I.; Siapi, E.; Lamprinidis, G.; Mikros, E.; Mavromoustakos, T. *Chem. Phys. Lip.* **2003**, *125*, 13.
- Zoumpoulakis, P.; Grdadolnik, G. S.; Matsoukas, J.; Mavromoustakos, T. *J. Pharm. Biomed. Anal.* **2002**, *28*, 125.
- Rognan, D. *Pers. Drug Dis. Des.* **1998**, *9-11*, 181.
- Tuccinardi, T.; Ferrarini, P. L.; Manera, C.; Ortore, G.; Saccomanni, G.; Martinelli, A. *J. Med. Chem.* **2006**, *49*, 984.
- Cramer, R. D. I.; Depriest, S.; Patterson, D.; Hecht, P. *The developing practice of comparative molecular field analysis*; Kubinyi, H., Ed.; ESCOM: Leiden, **1993**, 443.
- Klebe, G.; Abraham, U.; Mietzner, T. *J. Med. Chem.* **1994**, *37*, 4130.
- Mavromoustakos, T.; Kapou, A.; Benetis, N. P.; Zervou, M. *Drug Des. Rev. Online* **2004**, *1*, 235.
- Zoumpoulakis, P.; Mavromoustakos, T. *Drug Des. Rev. Online* **2005**, *2*, 537.
- Durdagi, S.; Papadopoulos, M. G.; Papahatjis, D. P.; Mavromoustakos, T. *Bioorg. Med. Chem. Lett.* **2007**, *17*, 6754.
- Brooks, B. R.; Brucoleri, R. E.; Olafson, B. D.; States, D. J.; Swaminathan, S.; Karplus, M. *J. Comp. Chem.* **1983**, *4*, 187.
- Sybyl Molecular Modeling Software Package*, ver. 6.8., Tripos Inc., St. Louis, MO 63144, 2001.
- Powell, M. J. D. *Math. Prog.* **1977**, *12*, 241.
- Gasteiger, J.; Marsili, M. *Tetrahedron* **1980**, *36*, 3219.
- Frisch, M. J.; Trucks, G. W.; Schlegel, H. B.; Scuseria, G. E.; Robb, M. A.; Cheeseman, J. R.; Zakrzewski, V. G.; Montgomery, Jr., J. A.; Stratmann, R. E.; Burant, J. C.; Dapprich, S.; Millam, J. M.; Daniels, A. D.; Kudin, K. N.; Strain, M. C.; Farkas, O.; Tomasi, J.; Barone, V.; Cossi, M.; Cammi, R.; Mennucci, B.; Pomelli, C.; Adamo, C.; Clifford, S.; Ochterski, J.; Petersson, G. A.; Ayala, P. Y.; Cui, Q.; Morokuma, K.; Malick, D. K.; Rabuck, A. D.; Raghavachari, K.; Foresman, J. B.; Cioslowski, J.; Ortiz, J. V.; Stefanov, B. B.; Liu, G.; Liashenko, A.; Piskorz, P.; Komaromi, I.; Gomperts, R.; Martin, R. L.; Fox, D. J.; Keith, T.; Al-Laham, M. A.; Peng, C. Y.; Nanayakkara, A.; Gonzalez, C.; Challacombe, M.; Gill, P. M. W.; Johnson, B.; Chen, W.; Wong, M. W.; Andres, J. L.; Gonzalez, C.; Head-Gordon, M.; Replogle, E. S.; Pople, J. A.; *Gaussian 98 Revision A.9*. Gaussian Inc., Pittsburgh PA, **1998**.
- Becke, A. D. *J. Chem. Phys.* **1993**, *98*, 5648.
- Hehre, W. J.; Ditchfield, R.; Pople, J. A. *J. Chem. Phys.* **1975**, *62*, 2921.
- Schuettelkopf, A. W.; van Aalten, D. M. F. *Acta Crystal* **2004**, *D60*, 1355.
- Lindhal, E.; Hess, B.; van der Spoel, D. *J. Mol. Model.* **2001**, *7*, 306.
- van Der Spoel, D.; Lindahl, E.; Hess, B.; Groenhof, G.; Mark, A. E.; Berendsen, H. J. *J. Comput. Chem.* **2005**, *26*, 1701.
- Berendsen, H. J. C.; Postma, J. P. M.; van Gunsteren, W. F.; Dinola, A.; Haak, J. R. *J. Comput. Chem.* **1984**, *5*, 3684.
- Essmann, U.; Perera, L.; Berkowitz, M. L.; Darden, T.; Lee, H.; Pedersen, L. G. *J. Chem. Phys.* **1995**, *103*, 8577.
- Humphrey, W.; Dalke, A.; Schulten, K. *J. Mol. Graphics* **1996**, *14*, 33.
- <http://www.microcal.com>.
- Soteriadou, K.; Tzinia, A. K.; Panou-Pamonis, E.; Tsikaris, V.; Sakarellos-Daitsiotis, M.; Sakarellos, C.; Papapoulou, Y.; Matsas, R. *Biochem. J.* **1996**, *313*, 455.
- Shim, J.-Y.; Welsh, W. J.; Howlett, A. C. *Biopolymers* **2003**, *71*, 169.
- Palczewski, K.; Kumasaka, T.; Hori, T.; Behnke, C. A.; Motoshima, H.; Fox, B. A.; Le Trong, I.; Teller, D. C.; Okada, T.; Stenkamp, R. E.; Yamamoto, M.; Miyano, M. *Science* **2000**, *289*, 739.